



Energy, Economic and Environmental (3E) Analysis of a Tank-in-Tank Solar Combisystem

Maryam Karami^{a,*}, Fatemeh Hami Saniabadi^a

^aDepartment of Mechanical Engineering, Faculty of Engineering, Kharazmi University, Tehran, Iran

Received: 2021-05-20

Accepted: 2021-08-10

Abstract

In this study, the thermal performance of a tank-in-tank solar combisystem is dynamically simulated to investigate the effect of various parameters such as collector type and area, storage tank volume, building specifications, heat exchange terminal units, and climatic conditions on system performance. The results showed that by increasing the collector area, tank volume and thickness of wall insulation, the solar fraction increases. It was also found that the use of floor heating instead of a radiator system improves the system performance. The solar fraction using the evacuated tube solar collector is 2.3% higher than that using flat plate solar collector. The annual solar fraction of 45.6%, 63.4%, 41.2%, 34%, 57.3% and 88.1% is obtained in Hot-Dry (Tehran), Hot-Dry (Yazd), Cold-Dry (Tabriz), Moderate-Humid (Rasht), Hot-semi Humid (Abadan), and Hot-Humid (Bandar Abbas), respectively. The environmental analysis indicates that using the proposed solar combisystem could save 2241.3 m³ natural gas and offsetting 4731.5 kg less CO₂ emissions during a year. The life cycle cost analysis shows that the payback time of the proposed system for the economic conditions of Iran is 7 years.

Keywords: Solar combisystem; Tank-in-tank; Economic analysis; Environmental analysis; Climatic conditions

Introduction

A solar combisystem (SCS) is a solar heating system which supply simultaneously domestic hot water (DHW) and space heating (SH) demands of residential buildings. SCSs normally consist of five sub-systems: solar collector loop, heat storage, heat distribution, controls, and auxiliary heaters. One key advantage of the SCS as compared to conventional solar water heaters is that SCSs increase the solar collector's utilization independent

of occupant hot water consumption because the heat collected by the solar collector also utilizes for the space heating.

Several studies have been done on thermal performance of the SCSs, of which different types has been categorised in the International Energy Agency Solar Heating and Cooling Programme (IEA), Task 26 [1]. By considering sizing, applicability, and average yearly system performance of SCSs, Lund [2] found the solar fraction in a SCS

*corresponding author: karami@khu.ac.ir

with a 50% usability, the solar fraction is 20–30% in Helsinki (60°N) and 25–40% in Vienna (48°N), respectively. The study by Letz et al. [3] indicates that fractional energy savings, with and without parasitic energy, can be expressed as a quadratic function of fractional solar consumption (FSC). Sustar et al. [4] compared the performance of the SCS with solar water heaters. They reported that the energy savings in the SCS is 27% higher than the solar water heater with 9 m² collector area. Using TRNSYS software, Papi et al. [5] examined the impact of various factors such as the climate, the load and size of main components as well as the heat source for the heat pump on system power consumption. The results showed that changes in collector area from 5 to 15 m² result in a decrease in system electricity of between 305 and 552 kWh/year. Asaee et al. [6] considered the potential of SCS in Canadian houses and found that a substantial fraction of the space heating, cooling and domestic hot water heating energy requirement of a simple house is provided in all major climatic regions of Canada. In the next study, they concluded that the reduction of fossil fuel consumption is affected by SCS more significant in comparison with electricity consumption [7]. Katsaprakakis and Zidianakis [8] computationally simulated a SCS, using annual time series of average hourly steps. It is seen that considering the high available solar radiation in school building in Crete, the proposed SCS can guarantee the 100% annual heating load coverage of the building, with an annual contribution from the solar collectors higher than 45%. The annually average thermal power production levelized cost is calculated at 0.15 €/kWh. Thapa et al. [9] designed, modeled, and optimized a SCS for typical single-family houses in Nepal (Terai and the Hilli region). The particle swarm optimization and the Hooke-Jeeves algorithms were combined to solve the optimization problem. Relative to the initial design, the life cycle cost is reduced by 66% and 77% for the Terai and the Hilli region, respectively. Karami and Javanmardi [10] investigated the performance of a SCS with two separate storage tanks for DHW and SH. Their results the maximum and minimum solar

fraction of the SCS occur in Cold-Dry and Hot-Humid Climate zones, respectively.

In this study, the thermal performance of a tank-in-tank SCS is dynamically simulated to investigate the effect of various parameters such as collector type and area, storage tank volume, building specifications, heat exchange terminal units, and climatic conditions on the system performance. Five different climate zones including Hot-Dry (Tehran), Hot-Dry (Yazd), Cold-Dry (Tabriz), Moderate-Humid (Rasht), Hot-semi Humid (Abadan), and Hot-Humid (Bandar Abbas) are selected for considering the effect of the climatic conditions on the system solar fraction. The environmental and economic impacts of the system are also analyzed for comprehensive investigation of the system performance.

2. System description and modelling

The schematic of tank-in-tank SCS is shown in Figure 1. The SCS configuration has one solar water tank (tank-in-tank) which provides the DHW and SH needs. The tank is charged by solar energy through solar collectors and if needed by auxiliary energy from boiler. Inner tank is dedicated to the DHW preparation, while the other is for the SH needs.

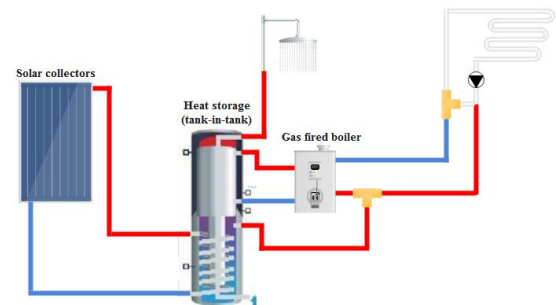


Figure 1. Schematic of tank-in-tank SCS

The simulation of the proposed SCS is done by T*SOL software, which is a program for designing and simulating solar thermal systems with hot water supply, space heating, swimming pool heating, process heat and large-scale systems. Solar components characteristics used to simulate SCS are listed in Table 1.

Table 1. System components characteristics

Table 1. System components characteristics			Tank		
Component	Parameter	Value			
Collector type	Flat plate	Volume Flow rate	72 (l/h)/ m ²	Fuel Type	Natural Gas
		Conversion Factor	80%	Nominal Power	22 kW
		Heat Transfer Coefficient	3.5 W/m ² k	DHW set-point Temperature	65°C
		Temperature Depending Heat Transfer Coefficient	0.015 W/m ² k ²	Max. Water Temperature	90°C
		Inc. Angle Modifier	90%	Supply Temperature	50°C
	Evacuated tube	Working Fluid	Water/EG (70%:30%)	Return Temperature	25°C
		Collector Area	28 m ²	Supply Temperature	70°C
		Inclination (tilt angle)	35.7	Return Temperature	40°C
		Glass Tube Diameter	65 mm		
		Glass Thickness	1.6 mm		
Storage Tank	Collector Length	1965 mm			
	Absorber Plate Material	Copper			
	Coating	Selective			
	Absorber Area	1.0 m ²			
	Inclination (tilt angle)	35.7			
	Tubes Direction	crosswise			
	Total Volume	2.1 m ³			
	Heat Loss Coefficient	0.16 W/m ² k			
	Inner DHW	280 lit			

Since one of the goals of this study is to investigate the impact of insulation thickness of building walls on solar fraction, the case study building is simulated in Design Builder. Figure 1 shows the modeling of the building in Design Builder. In the building external walls consist of 1.5 cm granite, 2 cm mortar, 20 cm brick and 3 cm gypsum from the outside to the inside, respectively. The roof or floor consists of 1 cm ceramic, 2 cm mortar, 31 cm cement block and 2 cm gypsum from top to bottom. Expanded polystyrene (EPS) as insulation material is selected. Other characteristics of the case study building are listed in Table 2. It should be noted that the rate of occupant's activity and the air infiltration into the building are calculated according to ASHRAE 90.1 [22]. The climate data such as sunlight, air flow rate, ambient temperature, humidity, etc. are calculated based on Tehran Mehrabad ASHRAE/ITMY file [23].

The solar fraction (F_{sol}) is defined as the ratio of energy supplied by solar energy to the required energy. Total solar fraction ($F_{sol,total}$), SH solar fraction ($F_{sol,DHW}$) and DHW solar fraction ($F_{sol,SH}$) are shown as below:

$$F_{sol,total} = \frac{Q_{CL}}{Q_{CL} + Q_{AUX,DHW} + Q_{AUX,SH}} \quad (1)$$

$$F_{sol,DHW} = \frac{Q_{CL} - Q_{S,HL}}{Q_{CL} - Q_{S,HL} + Q_{AUX,DHW}} \quad (2)$$

$$F_{sol,SH} = \frac{Q_{S,HL}}{Q_{S,HL} + Q_{AUX,HL}} \quad (3)$$

where Q_{CL} , $Q_{AUX,DHW}$, $Q_{AUX,SH}$ and $Q_{S,HL}$ are the energy output from the collector loop, the required DHW and SH auxiliary energy, and the SH demand.

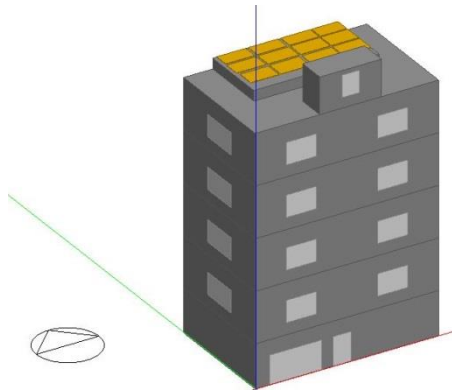


Figure 2. Modeling of the case study building in Design Builder

Table 2. System components characteristics

Parameter	Value
Number of floors	4
Floor area (m ²)	100
Window-to-Wall Ratio (WWR)	14%
Overall heat transfer coefficient of external walls	0.135 W/(m ² K)
Overall heat transfer coefficient of roof	0.1017 W/(m ² K)
Overall heat transfer coefficient of floor	0.118 W/(m ² K)
Overall heat transfer coefficient of windows	0.4 W/(m ² K)
Number of occupants in each floor	4
Occupant activity level	Seated, light work
Natural ventilation	1 AC/h
Infiltration	0.7 AC/h
Artificial lighting	5 W/m ²
Indoor design temperature (°C)	24
DHW demand (lit/day)	640
DHW set-point temperature (°C)	65

Window type	Double glazing
Total solar transmission	0.8

3. Results and discussion

The monthly variation of the ambient temperature and solar irradiation in Tehran is shown in Figure 3. The DHW and SH demands of the case study building is shown in Figure 4. As observed, the DHW demand varies between 812 kWh and 1272 kWh during the year. From November to March (warm season in Tehran), SH demand varies between 2287 kWh and 5371 kWh.

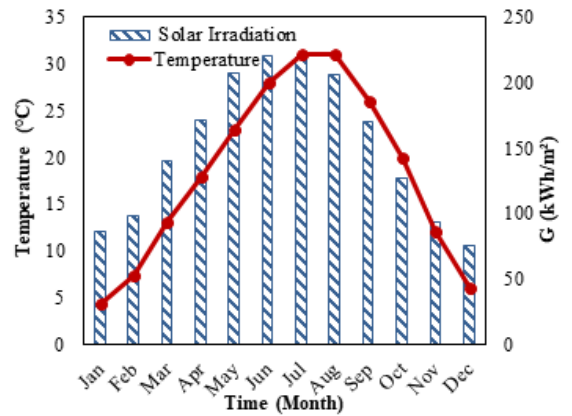


Figure 3. Monthly variations of ambient temperature and solar irradiation in Tehran

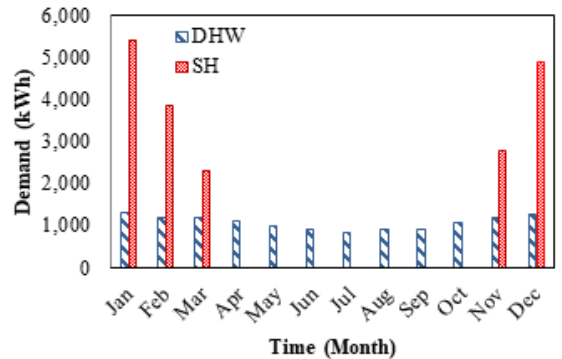


Figure 4. Monthly variation in DHW and SH demands of the building in Tehran.

The monthly variation of $F_{sol,DHW}$, $F_{sol,SH}$, and $F_{sol,total}$ of the tank-in-tank SCS is depicted in Figure 5. All DHW demand is supplied by the SCS in June and August; whereas, the $F_{sol,DHW}$ varies

from 61% to 99% in other months. The $F_{sol,SH}$ is obtained 26%, 11%, 13%, 17%, and 31% from November to March, respectively. Due to assign the greater portion of useful solar energy gain to provide DHW and higher SH demand than DHW, $F_{sol,DHW}$ is always higher than $F_{sol,SH}$. The minimum and maximum $F_{sol,total}$ are obtained 23% in January and 100% in June and August, respectively.

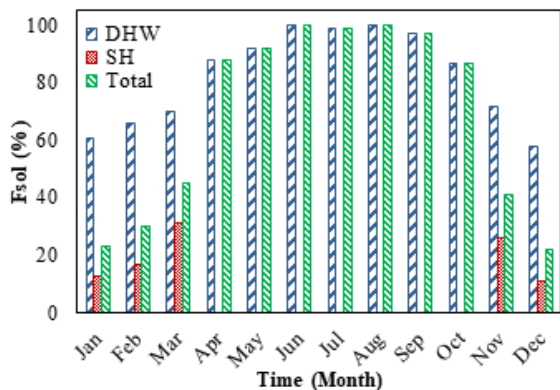


Figure 5. Monthly variation of DHW, SH and total solar fraction

3-1 Comparison with a heating buffer tank SCS

In Table 4, the performance of the tank-in-tank SCS is compared with a heating buffer tank SCS, which has two separate tanks for the DHW and SH. The DHW and SH tanks has the volume of 1000 l and 1100 l, respectively. The sum of tank volumes is equal to the tank-in-tank volume. It is interested to note that $F_{sol,SH}$ of the tank-in-tank SCS is approximately twice that of the heating buffer tank SCS, because the heat loss form the storage tanks in the tank-in-tank SCS is lower than that in the buffer tank SCS. On the other hand, the $F_{sol,DHW}$ of the heating buffer tank SCS is about 9.74% higher than that of the buffer tank SCS. This is because the useful energy gain is first allocated to the DHW tank and, then goes to the SH tank. The larger enhancement of $F_{sol,SH}$ shows the better performance of tank-in-tank SCS compared to buffer tank SCS.

Table 4. Performance comparison of the buffer tank and tank-in-tank SCSs

	Tank-in-Tank	Buffer tank
--	--------------	-------------

$F_{sol,DHW}$	81.31 %	91.05 %
$F_{sol,SH}$	17.29 %	8.82 %
$F_{sol,total}$	45.56 %	43.67 %

3-2 Effect of solar loop parameters

In Figure 6, the effect of the collector area on the solar fraction is plotted. As can be seen, by increasing the collector area from 5 m² to 50 m², the system $F_{sol,DHW}$, $F_{sol,SH}$ and $F_{sol,total}$ increase 58.3%, 28.4% and, 41.9% respectively. Considering the asymptotic trend of the Fsol variations by the collector area, it is concluded that increasing the collector area has a limit, beyond which there is no significant increase in the solar fraction. This is because by increasing the collector area, the solar absorption enhances, but the heat loss from the collector to the ambient also increases.

Figure 7 shows the $F_{sol,total}$ variation by the storage tank volume. As observed, by increasing the tank volume from 800 l to 4140 l, there is an increase in $F_{sol,total}$ from 37.7% to 48.9%. It should be noted that for higher tank volume of 3000 l, the Fsol enhancement decrease, because of higher thermal losses (due to larger surface area).

The system $F_{sol,total}$ using ETC as the solar collector is obtained 47.9% while it is obtained 45.6% using FPC. The vacuum envelope causes the decrease of the convection and conduction losses. Furthermore, the cylindrical absorber of ETC absorbed more solar radiation at low incidence angles and has the better performance throughout the day.

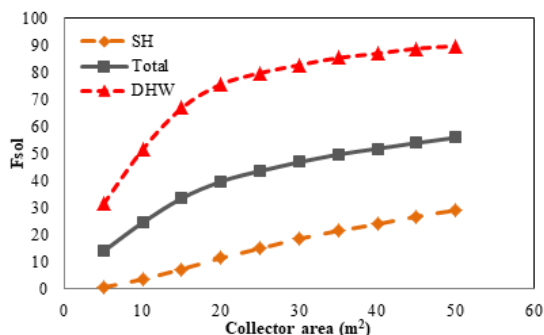


Figure 6. Effect of collector area on system solar fractions

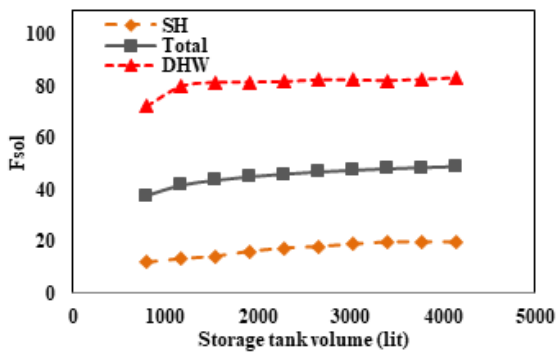


Figure 7. Effect of the storage tank volume on system solar fractions

3-2 Effect of building characteristics

The variation of the system $F_{sol,total}$ with different insulation thickness is presented in Table 5. The results show that by increasing insulation thickness, thermal conductivity decreases, so the building load decreases. Obviously, a lower building load results to a higher $F_{sol,total}$ for tank-in-tank SCS. For example, by increasing the insulation thickness of the external walls up to 22 cm, it is observed that the $F_{sol,total}$ increases about 9.8%.

Table 5. Effect of insulation thickness on $F_{sol,total}$

Building Type	Wall	Insulation thickness (cm)	U-Value (W/m^2K)	SH demand (kW)	F_{sol}
Case 1	External walls	27	0.135	14.64	45.6
	Floor	28	0.118		
	Roof	31	0.1017		
Case 2	External walls	9	0.342	18.41	39.9
	Floor	15	0.196		
	Roof	12	0.227		
Case 3	External walls	5	0.508	21.95	35.8
	Floor	2	0.546		
	Roof	3	0.494		

The effect of windows type on the system $F_{sol,total}$ is listed in Table 6. The results show that by increasing the windows U-Value from 0.4 W/m^2k to

2.8 W/m^2K , which is equals to the windows with lower thickness, the $F_{sol,total}$ decreases by 7.7% because of the increases of the heat loss trough windows.

Table 6. Effect of windows type on $F_{sol,total}$

Windows U-Value (W/m^2k)	SH demand (kW)	$F_{sol,total}$
0.4	14.64	45.6
1.4	16.99	41.8
2.8	20	37.9

The tank-in-tank SCS is simulated by three types of heat distribution units including floor heating, radiator and the combination of these two types, so that 50% of the load is supplied through the radiator and 50% through the underfloor system. The type of heat distribution units affects the energy consumption and thus, has impact on $F_{sol,total}$, which is shown in Table 7. The results show that the system $F_{sol,total}$ by using floor heating system is 2% higher than that by using the radiator. Using combined system, the $F_{sol,total}$ increases is 0.7%. The higher surface area of the floor heating system and the position of the tubes in this system improve its heating efficiency.

Table 7. Effect of heat distribution units type on $F_{sol,total}$

Heat Distribution Unit Type	$F_{sol,total}$
Floor Heating	45.6
FH + Rad (50:50)	44.1
Radiator	43.6

3-3 Effect of climatic conditions

In this study, the effect of climatic conditions on the solar fraction of an SCS is investigated considering five different climate zones: Hot-Dry, Cold-Dry, Moderate-Humid, Hot-semi- Humid, and Hot-Humid. Five sample cities of Iran including Yazd, Tabriz, Rasht, Abadan, and Bandar Abbas are selected from the climate zones, respectively. The system performance is also investigated in Tehran, the capital of Iran, with approximately 8.3 million populations and 3.3 million houses which have a great impact on the energy consumption in Iran [10].

The characteristics of the the climate zones are listed in Table 3.

Table 3. Geographic and climatic conditions of the selected cities [25]

Climate	Longitude (°E)	Latitude (°N)	Outdoor design temperature (°C)		Solar irradiation (KWh/m ² /day)
			Winter	Summer	
Hot-Dry (Tehran)	35.41	51.19	-4	40	5.2-5.4
Hot-Dry (Yazd)	54.4	31.9	-8	43	5.2-5.4
Cold-Dry (Tabriz)	46.27	38.1	-11	35	3.8-4.5
Moderate-Humid (Rasht)	49.59	37.27	-3	32	2.8-3.8
Hot-semi Humid (Abadan)	48.29	30.35	3	47	3.8-5.4
Hot-Humid (Bandar Abbas)	56.27	27.18	9	51	4.5-5.2

Based on the results of Figure 7, the $F_{sol,total}$ is obtained 88.1%, 63.4%, 57.3%, 45.6%, 41.2%, and 34% in cities of Bandar Abbas, Yazd, Abadan, Tehran, Tabriz, and Rasht, respectively. The maximum $F_{sol,total}$ is obtained in climate zone of Hot-Humid (Bandar Abbas) and the minimum one is obtained in Moderate-Humid (Rasht) due to low solar radiation. In Hot-Dry cities (Tehran, Yazd) with high solar radiation, $F_{sol,total}$ is lower in comparison with Hot-Humid (Bandar Abbas) because of the lower temperatures during the night and the larger heat loss from the tank. In cities of Bandar Abbas, Yazd, Abadan, Tehran, Tabriz, and Rasht the $F_{sol,DHW}$ is obtained 94.8%, 91.3%, 85.5%, 81.3%, 74.9%, and 59.7%, and the $F_{sol,SH}$ is obtained 56.8%, 25%, 20.3%, 17.3%, 17.5%, and 9.5%, respectively.

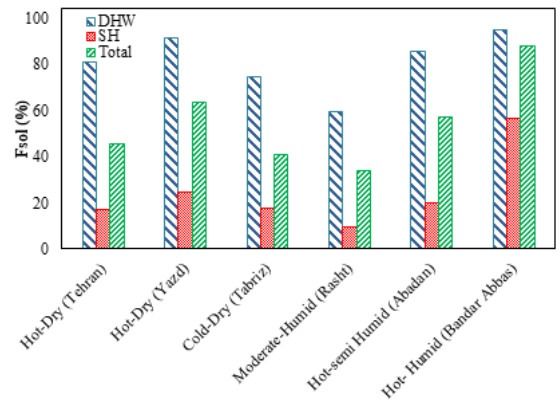


Figure 8. Effect of climatic conditions on $F_{sol,total}$

4. Economic analysis

The method employed in this study for the economic analysis is life cycle cost (LCC) analysis. This method considered the time value of money and the complete range of costs [11]. The total cost of the solar equipment (C_s) is given by:

$$C_s = C_A A_c + C_I \tag{4}$$

Where A_c , C_A and C_I are the collector area, the collector area-dependent costs and the collector area-independent costs, respectively.

The integrated cost of the auxiliary energy use for the first year, that is, solar backup, is given by the formula:

$$C_{AUX} = C_{FA} \int_0^t L_{AUX} dt \tag{5}$$

The integrated cost of the total load for the first year, that is, the cost of conventional fuel without solar energy, is:

$$C_L = C_{FL} \int_0^t L dt \tag{6}$$

where C_{FA} and C_{FL} are cost rates (\$/GJ) for auxiliary energy and conventional fuel, respectively.

The present worth of an cost (C) at the end of year (n) is:

$$PW_n = \frac{C(1+i)^{n-1}}{(1+d)^n} \tag{7}$$

Where d and I are discount and interest rates, respectively.

The total present worth (TPW), is given by:

$$TPW = C \left[\sum_{i=1}^n \frac{(1+i)^{j-1}}{(1+d)^j} \right] = C[PWF(n, i, d)] \tag{8}$$

The present worth of life cycle solar savings (LCS) is calculated as follows:

$$PW_{LCS} = \sum_{j=1}^n \frac{\text{Solar energy savings}}{(1+d)^j} \quad (9)$$

Payback time (n_p) is given by the following:

$$n_p = \frac{\ln\left(\frac{C_s(i_F - d)}{FLC_{F1}} + 1\right)}{\ln\left(\frac{1+i_F}{1+d}\right)} \quad (10)$$

where F_{sol} , L , C_{F1} and i_F are solar fraction, load (GJ), first year unit energy cost delivered from fuel (\$/GJ) and fuel inflation rate, respectively.

In this study, the period of economic analysis is equivalent to the life of the system, which is taken as 20 years. According to Table 8, the total cost of system is 8152.7 \$. Installation cost and extra insurance, maintenance and parasitic cost is considered to be 1% and 0.6% of component cost. The inflation and discount rates are considered equal to the Iran's economic indicators for 2016, which were respectively 9.6% and 15% [12]. The energy carriers including the natural gas and electricity in Iran are subsidized by the Government; however, in this analysis, the non-subsidized global prices are considered. The natural gas price is considered $0.7715 \frac{\$}{m^3}$ [13]. Annual inflation rate of natural gas price is expected to be 15%. The total LCS of 11222.8 \$ and the payback period of 6 years confirms that the SCS system is an appropriate option to supply the energy demand of the residential buildings.

Table 8. Cost of solar system

Component	Cost (\$)
Flat plate collectors	2100
Storage tank	5135
Boiler	817
Pump	20
Installation cost	80.72
Insurance, maintenance and parasitic cost	48.432

5. Environmental analysis

Burning of fossil fuels to generate the energy to provide heat for SH and DHW will result in harmful gas emissions whose elimination from the environment is so much costly. Using an SCS can reduce the greenhouse gas (GHG) emissions. The fuel type that is used for boiler in this study is natural gas. Figure 9 indicates the monthly variation in natural gas savings and reduction of CO₂ emission. The minimum natural gas savings is obtained 154 m³ in December due to low $F_{sol,total}$ and the maximum is obtained 201 m³ in June. Furthermore, the minimum reduction of CO₂ emission is obtained 326 kg in December and the maximum is obtained 424 kg in June. The annual natural gas savings of 2241.3 m³ and annual reduction of CO₂ emission of 4739.45 kg is obtained for tank-in-tank SCS.

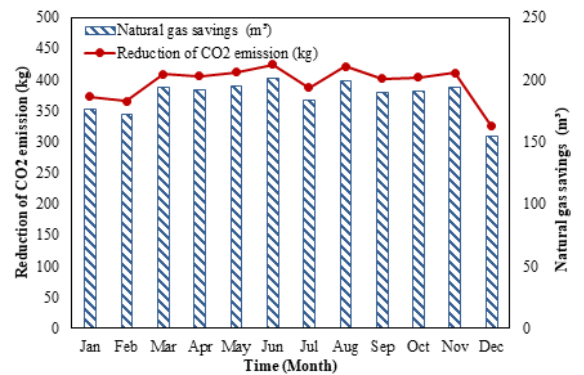


Figure 9. Environmental impacts of the system

6. Conclusion

In this study, the performance of a tank-in-tank SCS is dynamically investigated and the effect of various parameters on the system solar fraction is evaluated. The findings can be summarized as follows:

- By increasing the collector area from 5 to 50 m², the $F_{sol,total}$ increases from 13.9% to 55.8%.
- By increasing the volume of the storage tank from 800 to 4140 lit, the $F_{sol,total}$ increases from 37.7% to 48.9%.
- In building, by increasing insulation thickness, building load decreases and the F_{sol} increases.
- Changing the system heat distribution elements type from radiator to underfloor heating increases the F_{sol} by 2%.
- In considering SCS, using ETC instead of FPC increases the F_{sol} by 2.3%
- The annual $F_{sol,total}$ is obtained 88.1%, 63.4%, 57.3%, 45.6%, 41.2%, and 34% in cities of Bandar Abbas, Yazd, Abadan, Tehran, Tabriz, and Rasht, respectively.
- The annual natural gas savings and reduction of CO₂ emission is obtained 2241.3 m³ and 4739.45 kg, respectively.

Nomenclature

A : Area, m²

C: Cost, \$

d: Discount rate

F: Solar fraction

L: Load, J

i: Inflation rate

n: Number of years

Q: Heat, J

t: time, s

Subscripts

AUX: Auxiliary

FA: Auxiliary fuel

FL: Load fuel

S: Solar equipment

F: Fuel

P: Payback

References

- [1] IEA, 2002. Task 26: Solar combisystems. International Energy Agency –Solar Heating and Cooling Programme, 2002.
- [2] P.D.Lund, *Sizing and applicability considerations of solar combisystems*. Solar Energy, 2005.**78**: p. 59-71.

[3] T. Letz, C. Bales, B. Perers, *A new concept for combisystems characterization: The FSC method*. Solar Energy, 2009. **83**: p. 1540–1549.

[4] J. L. Sustar, J. Burch, M. Krarti, *Performance modeling comparison of a solar combisystem and solar water heater*, Journal of Solar Energy Engineering, 2015. **137**: p. 061001-1:7.

[5] S. Poppi, C. Bales, M. Y. Haller, A. Heinz, *Influence of boundary conditions and component size on electricity demand in solar thermal and heat pump combisystems*, Applied Energy, 2016. **162**: p. 1062-1073.

[6] S. R. Asaee, V. Ismet Ugursal, Ian Beausoleil-Morrison, Nouredine Ben-Abdallah, *Preliminary study for solar combisystem potential in Canadian houses*. Applied Energy, 2014. **130**: p.510–518.

[7] S. R. Asaee, V. I. Ugursal, I. Beausoleil-Morrison, *Techno-economic study of solar combisystem retrofit in the Canadian housing stock*. Solar Energy, 2016. **15**: p. 426–443.

[8] D. A. Katsaprakakis, G. Zidianakis, *Optimized dimensioning and operation automation for a solar-combi system for indoor space heating. A case study for a school building in Crete*. Energies, 2019. **12**: p. 177-188.

[9] B. Thapa, W. Wang, W. Williams, *Life Cycle Cost Optimization of a Solar Combisystem in Nepal*. Journal of Asian Architecture and Building Engineering, 2021.

[10] Karami M., Javanmardi F., *Performance assessment of a solar thermal combisystem in different climate zones*, Asian Journal of Civil Engineering, 2020. **21**: p.751–762.

[11] S.A. Kalogirou, *Solar Energy Engineering: Processes and Systems*, Second Edition, Elsevier Inc., 2014.

[12] Central bank of the Islamic Republic of Iran.

[13] Tyra B. Electric Power Monthly with Data, U.S. Energy Inf. Adm. 2019; July: p.1–772.